Specific Mutation Near the Primary Donor in Photosystem I from *Chlamydomonas reinhardtii* Alters the Trapping Time and Spectroscopic Properties of P_{700}[†]

Alexander N. Melkozernov,[‡,§] Hui Su,[§,||] Su Lin,[‡,§] Scott Bingham,[§,||] Andrew N. Webber,[§,||] and Robert E. Blankenship*[,‡,§]

Department of Chemistry and Biochemistry and Center for the Study of Early Events in Photosynthesis, Arizona State University, Tempe, Arizona 85287-1604, and Department of Botany, Arizona State University, Tempe, Arizona 85287-1601

Received September 4, 1996; Revised Manuscript Received December 16, 1996[⊗]

ABSTRACT: Time-resolved absorption and fluorescence spectroscopy were used to investigate the energy and electron transfer processes in the detergent-isolated photosystem I core particles from the site-directed mutant of *Chlamydomonas reinhardtii* with the histidine-656 of PsaB replaced by asparagine [HN(B656) mutation]. The specific mutation near the primary donor molecule results in a 40 mV increase in the P_{700}/P_{700}^+ midpoint potential [Webber, A. N., Su Hui, Bingham, S. E., Käss, H., Krabben, L., Kuhn, M., Jordan, R., Schlodder, E., & Lubitz, W. (1996) *Biochemistry 35*, 12857−12863]. There is no indication that the HN(B656) mutation affects the spectral distribution of the antenna pigments. However, the lifetime of the trapping process measured independently by transient absorption and fluorescence spectroscopy in the mutant PSI core antenna is increased by a factor of approximately 2 (∼65 ps compared to ∼30 ps in the wild-type PSI). This implies that the trapping process in the PSI antenna is limited by the process where the primary donor molecule directly participates. The HN(B656) mutation results in the appearance of a new bleaching band at 670 nm in the spectrum which is due to formation of P_{700}^+ upon photooxidation. The difference spectrum of the photoreduction of the possible primary acceptor, A_0 in the mutant PSI is very similar to wild type, indicating that it is unaffected by the HN(B656) mutation. Possible mechanisms for slowing of the trapping process and the appearance of a new band in the $P_{700} - P_{700}^+$ difference spectrum of the HN(B656) PSI are discussed.

Photosystem I is an integral membrane pigment−protein complex that uses light energy to transfer electrons from plastocyanin to ferredoxin. The primary electron donor, P_{700},[1] and early electron acceptors A_0, A_1, and F_X are coordinated by a heterodimer of the PsaA and PsaB subunits. PsaA and PsaB also harbor approximately 80−100 molecules of Chl *a* that serve as an antenna to transfer excitation energy to P_{700} (Golbeck & Bryant, 1991). Recently, time-resolved spectroscopic studies have revealed a general picture for the primary steps of electron transfer in PSI reaction centers. The excited primary donor molecule, P_{700}*, transfers an electron to the primary acceptor, A_0, in ∼1−4 ps (Holzwarth et al., 1993; Hastings et al., 1994b; Kumazaki et al., 1994a; White et al., 1996). A_0 is then reoxidized by the secondary electron acceptor A_1, a phylloquinone molecule, in ∼20−50 ps (Shuvalov et al., 1986; Hastings et al., 1994b; Kumazaki et al., 1994a,b; Hecks et al., 1994). The A_1 acceptor transfers an electron to the [4Fe-4S] iron−sulfur center F_X, the terminal electron acceptor, within the PSI core (Moënne-Loccoz et al., 1994). The F_A and F_B iron−sulfur clusters are located on a separate subunit, PsaC (Golbeck & Bryant, 1991). The recent 4.5 and 4 Å resolution X-ray structure models of cyanobacterial PSI (Fromme et al., 1996; Krauss et al., 1996) support the models of electron transfer reactions in PSI RCs based on spectroscopic investigations. The crystal structure indicates the presence of two potential electron transfer pathways, each consisting of two monomeric Chls that lie on either side of the C_2 symmetry axis running through F_X, on the stromal side, and P_{700}, on the lumenal side of PSI. The monomeric Chls furthest from P_{700} are thought to be A_0. The functions of two additional Chls are unknown. It was suggested that these molecules participate in mediating electron transfer from P_{700} to A_0 (Hastings et al., 1995a).

Extensive spectroscopic investigation has shown that PSI antenna energy transfer processes include several phases with different lifetimes: (i) fast energy transfer within a pool of Chl molecules (∼0.2 ps) (Du et al., 1993); (ii) energy equilibration process between different pools of Chls (2−8 ps) (Klug et al., 1989; Du et al., 1993; Holzwarth et al., 1993; Turconi et al., 1993; Hastings et al., 1994a, 1995b; DiMagno et al., 1995); (iii) energy transfer from the antenna to P_{700} (20−40 ps) (Owens et al., 1988; Holzwarth et al., 1993; Hastings et al., 1994a, 1995a,b). However, data obtained

[†] This work was supported by NSF Grant MCB 9418415 to R.E.B. and by National Research Initiatives Competitive Grants Program Grant 95373062044 to A.N.W. This is Publication No. 319 from the Arizona State University Center for the Study of Early Events in Photosynthesis.

* To whom correspondence should be addressed at the Department of Chemistry and Biochemistry, Arizona State University, Tempe, AZ 85287-1604. Phone: (602)965-1439. Fax: (602)965-2747. Email: Blankenship@asu.edu.

[‡] Department of Chemistry and Biochemistry.

[§] Center for the Study of Early Events in Photosynthesis.

[||] Department of Botany.

[⊗] Abstract published in *Advance ACS Abstracts,* February 15, 1997.

[1] Abbreviations: A_0, primary electron acceptor in PSI; A_1, secondary electron acceptor in PSI; B(Chl) *a*, bacterio(chlorophyll) *a*; B(Pheo), bacterio(pheophytin); Chl *b*, chlorophyll *b*; *β*-DM, *β*-dodecyl maltoside; TX100, Triton X-100; DAS, decay-associated spectrum (spectra); FWHM, full-width at half-maximum PMS, phenazine methosulfate; PSI, photosystem I; P_{700}, primary electron donor in PSI; PsaB, PsaB protein of PSI core; F_X, $F_{A,B}$, iron−sulfur clusters of PSI; His-656, a histidine, the 656th amino acid residue of PsaB; HN(B656), mutation with His-656 of PsaB replaced by Asn.

S0006-2960(96)02235-0 CCC: $14.00

by time-resolved transient absorption and fluorescent spectroscopy are complicated by overlapping of the spectral signatures of heterogeneous antenna and reaction center Chl *a* molecules. Therefore, it is difficult for these investigations to develop an appropriate model for the migration of excitation energy in the PSI core antenna. The existing models are based upon alternative assumptions that energy migration from the photosynthetic antenna to P_{700} is limited by either the primary charge separation step, termed the trap-limited model (Pearlstein, 1982; Trissl, 1993), or a bottleneck process in the antenna, termed the diffusion-limited model [see Sundström and van Grondelle (1995) and references cited therein]. The special trap-limited model assumes that energy transfer from "red" pigments absorbing light at the long-wavelength spectral region to P_{700} is a limiting step (van Grondelle & Sundström, 1988; Otte et al., 1993).

Recent success in transformation of the chloroplast genome in *Chlamydomonas reinhardtii* has allowed specific mutations to be generated in the vicinity of P_{700} (Krabben et al., 1995; Webber et al., 1996). Using site-directed mutagenesis, His-656 of PsaB was replaced by either asparagine or serine (Webber et al., 1996). It was shown that both mutations result in a 40 mV increase in the midpoint potential of P_{700}/P_{700}^+ as well as significant changes in the $P_{700}^+ - P_{700}$ difference spectra and ^{1}H ENDOR spectra of P_{700}^+. Histidine-656 is located in membrane span X of PsaB and has been proposed as a possible ligand to P_{700} (Cui et al., 1995; Webber, et al., 1996).

If the energy transfer from antenna Chls to the reaction center in PSI is best described by a trap-limited model (Laible et al., 1994) in which the excitation lifetime in the antenna system is directly proportional to the intrinsic time of the primary charge separation step, then mutations that shift the P_{700} midpoint potential would be expected to result in a change in the trapping time. To address this issue, we used time-resolved absorption and fluorescence spectroscopy to investigate the energy and electron transfer processes in wild-type and HN(B656) mutant of PSI from *C. reinhardtii*. We show that substitution of His-656 for Asn results in a decrease of the trapping rate by a factor of 2 and in the appearance of a new bleaching band at 670 nm in the difference spectrum that is attributed to absorbance changes upon P_{700}^+ formation. The $A_0^- - A_0$ difference spectrum obtained after reduction of secondary electron acceptors in HN(B656) RC resembles the same spectrum from the wild-type RC, indicating that the mutation apparently does not affect the primary acceptor molecule.

MATERIALS AND METHODS

Strains. Specific mutagenesis of PsaB and chloroplast transformation of the PSII-less FuD7 strain of *C. reinhardtii* (Bennoun et al., 1986) were performed as previously described (Webber et al., 1996). In this work, we follow the designations of Webber et al. for a recipient FuD7 strain as wild type and the site-directed mutant in which His-656 of the PsaB subunit is replaced by Asn as HN(B656).

PSI Isolation. PSI particles from both wild type and the HN(B656) strain of *C. reinhardtii* were isolated using detergents β-DM or TX100 and sucrose density centrifugation according to protocols described previously (Takahashi et al., 1991). The Chl *a*/*b* ratio in PSI preparations was >2. Chl *a* concentration in PSI preparations was determined using the extinction coefficient of 60 mM^{-1} cm^{-1} at 677 nm (Thornber, 1969). The Chl *a*/P_{700} ratio was calculated using a differential extinction coefficient of 64 mM^{-1} cm^{-1} (Hiyama & Ke, 1972) for P_{700} oxidation. In our experiments, we used PSI preparations with different antenna sizes varying from 100 to 30 Chl *a* per P_{700}.

Picosecond Transient Absorption Spectroscopy. For measurements of time-resolved absorption spectra the samples of PSI from wild type and HN(B656) mutant of *C. reinhardtii* were treated under the following conditions:

(1) Neutral Conditions. The sample was suspended in 20 mM Tris-HCl buffer, pH 8.0, containing 20 mM sodium ascorbate and about 10 μM PMS. Under these conditions, the laser flash induced charge separation between the primary electron donor and electron acceptors occurs in the open PSI reaction centers, followed by charge recombination between P_{700}^+ and photoreduced iron−sulfur centers F_X or $F_{A,B}$ with a lifetime of 1−2 ms or 30 ms, respectively (Golbeck & Bryant, 1991). Prior to each experiment under neutral conditions, the kinetics of P_{700} photobleaching and re-reduction were measured using a millisecond flash spectrometer as described further under Materials and Methods. The concentration of PMS was adjusted to ensure complete rereduction of P_{700}^+ in less than 30 ms, and was typically 10 μM.

(2) Reducing Conditions. The sample was suspended in 200 mM glycine buffer, pH 11.0, containing 20 mM sodium ascorbate and 10 μM PMS. After degassing, sodium dithionite was added to the sample to a final concentration of 30 mM. Under these highly reducing conditions, the secondary electron acceptor A_1 is doubly reduced, and the iron−sulfur complexes F_X and $F_{A,B}$ are reduced. This reduction blocks electron transfer in the RC so that the radical pair $P^+A_0^-$ forms and then recombines with a lifetime of 30−50 ns (Mathis et al., 1988; Sétif & Bottin, 1989; Kleinherenbrink et al., 1994).

Following treatment, the sample was loaded in a spinning cell with an optical path length of 2 mm and a diameter of 12 mm. The rotating rate of the cell and recombination times of reduced acceptors with P_{700}^+ were adjusted to prevent the accumulation of P^+ during the measurements. The absorbance of the sample in the cell was ∼1−1.2 at the peak of the Q_y absorption band at 677 nm.

The optical setup of the laser system was described earlier (Lin et al., 1995). The final output optical pulses from the laser and amplifier system were 200 fs FWHM at 590 nm, 20 μJ, at a repetition rate of 540 Hz. The 590 nm beam was split into two parts. One part was used as a pump beam and was focused on a rotating quartz plate to generate a white light continuum, which was passed through a 700 nm interference filter (FWHM ∼10 nm). The beam was reamplified by a prism dye amplifier with dye LDS 698 (Exciton) pumped by a 532-nm beam from the regenerative amplifier. Another part of the 590 nm beam was used as a probe beam and was focused on a 1 cm water flowing cell to generate a white light continuum which was selected by using a long-pass filter. The polarization of the probe beam was set at the magic angle with respect to the polarization of the pump beam. Under low intensity excitation, a reaction center was excited by less than one photon. Such a low level of excitation minimized the singlet−singlet annihilation processes in PSI antenna.

Transient absorption spectra were measured with different time delays on −10−90 ps or −20−180 ps time scales in the 640−780 nm spectral region. Spectra were taken with a wavelength resolution of 0.14 nm/channel and were averaged over 15 channels to obtain a wavelength resolution of 2 nm. Transient absorption difference kinetics measured in the 640−750 nm spectral region were analyzed globally, assuming multiexponential kinetics. The quality of the fit was judged by the plots of residuals.

Time-Resolved Fluorescence Measurements. The fluorescence lifetimes of the PSI core antenna were measured using time-correlated single-photon counting as described previously (Causgrove et al., 1990). The excitation wavelength was at 590 or 682 nm. The optical density of the samples at 677 nm was <0.3. We did not flow the sample through the cuvette. Under these conditions, and the 3.8 MHz repetition rate of laser pulses, all reaction centers were in the closed state (P_{700} oxidized). Previous studies have shown that the kinetics of fluorescence decay in the antenna of PSI from *C. reinhardtii* are independent of the redox state of PSI (Owens et al., 1988; Holzwarth et al., 1993; Hastings et al., 1994a).

The PSI core antenna fluorescence decay kinetics were measured in the 650−740 nm spectral region. After deconvolution of the fluorescence decay kinetics with measured instrument response function (FWHM ∼40 ps), the result was fit to a sum of exponential components. The quality of the fits was assessed using a reduced χ^2 criterion and plots of weighted residuals. Decay-associated spectra were constructed after global analysis in the 650−740 nm spectral region. The time resolution of the instrument was 5 ps per channel.

Millisecond Flash-Induced Spectroscopy. Flash-induced absorbance difference changes of PSI particles on the millisecond time scale were measured using the instrument described earlier (Kleinherenbrink et al., 1994). Radical pair recombination after a saturating 532 nm laser flash was monitored for each PSI preparation at 694 nm. Before the picosecond absorption experiments, the $P_{700}^+ - P_{700}$ difference spectrum of each sample was measured in the spectral region where transient absorption measurements were performed.

RESULTS

Transient Absorption Measurements under Neutral Redox Conditions. Figure 1 shows the time-resolved absorption difference spectra measured on the 180-ps time scale for the open PSI from the wild type (A) and HN(B656) mutant (B) of *C. reinhardtii* under low intensity laser excitation at 700 nm.

In wild type, the difference spectrum taken at 4 ps (Figure 1A) is characterized by a bleaching centered at 686 nm caused by the excitation of antenna Chl *a* molecules. The 30-ps spectrum represents a recovery of this excitation in the antenna and has a peak at 691 nm with a shoulder at 680 nm. The 30-ps spectrum has contributions from absorption changes associated with the decay of excitation energy in the PSI antenna and P_{700} photooxidation.

The 70-ps and 180-ps spectra have similar shapes within experimental error. Both spectra show bleaching bands at 680 and 693 nm. This indicates that the initial decay processes in wild type PSI are completed within the first 70 ps and that the 70- and 180-ps spectra represent the processes nondecaying on the time scale considered here.

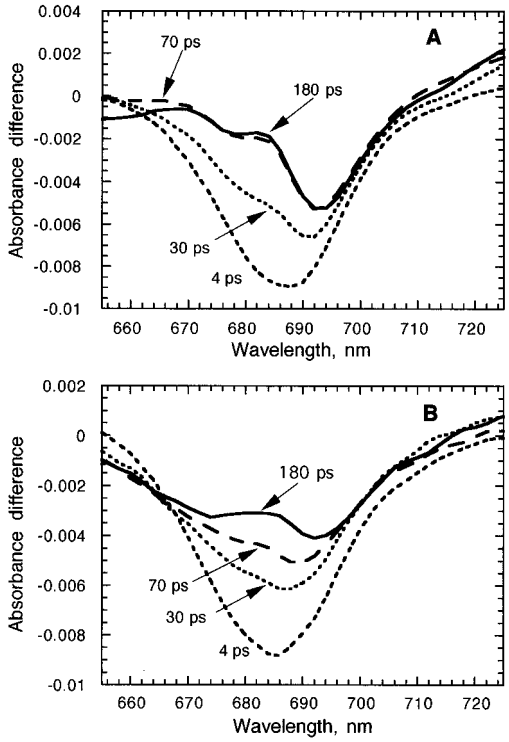

FIGURE 1: Time-resolved transient absorption spectra of detergent-isolated PSI from wild type (A) and HN(B656) mutant (B) of *C. reinhardtii* under neutral conditions at room temperature after laser excitation at 700 nm (FWHM = 10 nm). Spectra measured at 4-, 30-, 70-, and 180-ps time delay on the 0−180 ps time scale. Chl/P_{700} ∼ 60 in both preparations.

We performed time-resolved measurements for PSI from the HN(B656) mutant of *C. reinhardtii* under similar neutral conditions and low intensity excitation at 700 nm. The data were collected at different delay times on both the 90- and 180-ps time scales. Transient absorption spectra measured at 4, 30, 70, and 180 ps after the laser pulse are shown in Figure 1B.

The 4-ps spectrum is characterized by photobleaching in the 650−710 nm spectral region. This spectrum resembles the 4-ps spectrum of wild type PSI in Figure 1A and represents the appearance and decay of excitations of Chl antenna molecules absorbing in that spectral region. The 2 nm blue shift of this spectrum as compared to the 4-ps spectrum of wild type PSI is within wavelength resolution.

The shape of the 30-ps and 70-ps spectra in Figure 1B resembles the 30-ps spectrum of wild type PSI. The ratio of the amplitude of absorbance changes (ΔA) at 690 nm of the 70-ps spectrum to the ΔA amplitude at 692 nm of the 30-ps spectrum in the wild type PSI is less than in the HN(B656) mutant PSI.

The 180-ps spectrum in Figure 1B is different from the 180-ps spectrum of wild type PSI (Figure 1A). It is characterized by photobleaching at 692 nm and a broad photobleaching at the 660−685 nm region which is due to contributions from the photobleaching band at 680 nm and a new band around 670 nm. The ratio of the ΔA amplitude at 686 nm in the 4-ps spectrum to the ΔA amplitude at 692 nm in the 180-ps spectrum is higher than in the wild type spectra (Figure 1A). These spectral changes result from the HN(B656) mutation. The difference in the position of

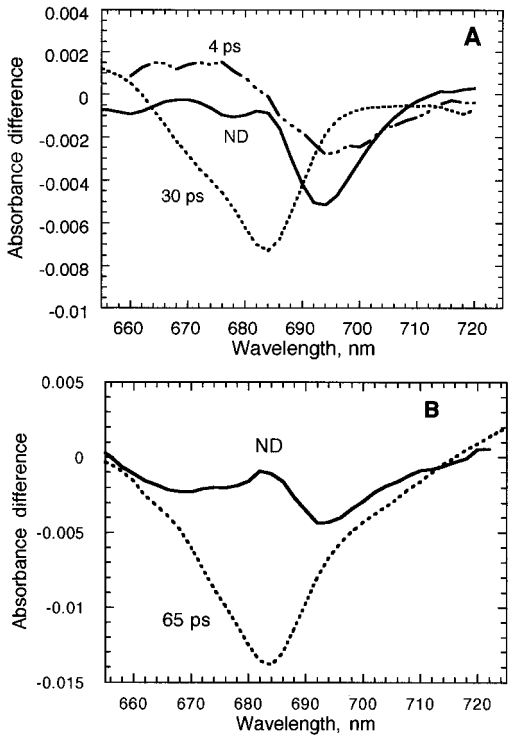

FIGURE 2: Decay-associated spectra of exponential components obtained by global analysis of transient absorption kinetics upon excitation at 700 nm for detergent-isolated PSI from wild type (A) and HN(B656) mutant (B) of *C. reinhardtii* collected on the 0−180 ps time scale. The 4-ps DAS in panel A was obtained by the global analysis of data collected on the 0−90 ps scale and was normalized for the optical density of the sample. ND, nondecaying.

maximum of photobleaching in the 180-ps spectrum of HN-(B656) mutant, PSI, as compared to that in wild type spectra, is not considered to be significant.

Transient absorption difference kinetics measured on a 90-ps and 180-ps time scale in the 650−750 nm spectral region for PSI from wild type and HN(B656) mutant of *C. reinhardtii* were fit by global analysis. Decay-associated spectra obtained for every time scale were checked for consistency with each other using plots of weighted residuals. Figure 2A displays DAS of exponential components obtained from the global analysis of data collected on a 180-ps scale under neutral conditions in PSI from wild type (Chl *a*/P_{700} ratio ∼60). The best fit was obtained for the one-exponential component and a nondecaying component on the 180-ps scale.

On the 90-ps scale, a fast decay component with a lifetime of 4 ps for the same particles was resolved. This component is also shown in Figure 2A. The 4-ps DAS displays a peak with positive amplitude at 675 nm and a peak with negative amplitude at 695 nm. The shape of this component is in good agreement with the shape of 4-ps DAS obtained earlier for detergent-isolated cyanobacterial PSI under 710 nm excitation (Hastings et al., 1995b) and is indicative of energy transfer from a pool of chlorins absorbing light in the region of 695−710 nm to the chlorins absorbing light around 680 nm.

The DAS of the fast component with a lifetime ∼30 ps has a negative peak at 684 nm. The shape of this component is similar to the shape of the 21-ps DAS we obtained from the measurements of transient absorption spectra of TX100-isolated PSI from a Chl *b*-less strain of *C. reinhardtii* (data not shown) and to the 22.4-ps DAS reported earlier for *β*-DM-isolated PSI particles from a Chl *b*-less strain of *C. reinhardtii* (Hastings et al., 1995a). In different sets of experiments using excitation at 675 and 700 nm, we measured transient absorption spectra of wild type PSI on a 90-ps time scale and obtained similar results (data not shown). The shape and the lifetime of this exponential component were independent of excitation wavelength. The same was reported for PSI from cyanobacteria and higher plants (Hastings et al., 1994a, 1995a). This 20−35 ps phase of PSI core antenna decay in cyanobacteria, higher plants, and green algae was previously attributed to the overall decay of excitations in antenna due to the trapping process (Holzwarth et al., 1993; Turconi et al., 1993; Hastings et al., 1994a, 1995a,b).

The nondecaying spectrum in Figure 2A represents the processes decaying on a nanosecond or longer time scale and is constant on the time scale considered here. The spectral profile of this component is similar to that of difference spectra taken at time delays within the 70−180 ps region (see 70- and 180-ps spectra in Figure 1A). Figure 2B shows the decay-associated spectra obtained by the global analysis of the HN(B656) data set on a 180-ps time scale. PSI particle of the HN(B656) mutant contain ∼60 Chl *a* per P_{700}. The best description of the data was obtained for the one-exponential component with lifetime ∼65 ps and a nondecaying component. We did not resolve the fast energy equilibration component for the mutant PSI preparations on both the 180-ps and the 90-ps time scale (data not shown).

The 65-ps DAS in the HN(B656) mutant PSI has a negative peak at 684 nm, and the shape of this spectrum is very similar to the shape of the 30-ps DAS in the wild type PSI preparations. This component reflects the overall decay of excitations in PSI antenna due to trapping by the reaction center. The change in the trapping time of PSI core antenna from HN(B656) mutant might be determined by the change of the properties of the trap, the primary donor molecule P_{700}. In the Discussion, we show that this is consistent with a trap-limited model of PSI excited dynamics.

The long-lived component from the fitting of HN(B656) PSI data in Figure 2B shows bleaching at 692 nm and the appearance of the new band at 670 nm. The shape of this component is different from the shape of the nondecaying spectrum obtained for wild type PSI (Figure 2A). The appearance of this new band in the nondecaying spectrum in Figure 2B is a result of substitution of His-656 in PsaB of PSI for Asn.

Table 1 summarizes the lifetimes of the fast component reflecting the trapping process obtained by global analysis of picosecond transient absorption data for different PSI preparations from both wild type and HN(B656) mutant of *C. reinhardtii*. The average lifetime for this component measured by picosecond transient absorption spectroscopy using excitation at 700 nm on the 90- and 180-ps time scales in different wild type PSI preparations was 26 ± 5 ps. The Chl *a*/P_{700} ratio for PSI particles from HN(B656) mutant used in our experiments was ∼60−80. The average trapping time measured by picosecond transient absorption spectroscopy for different PSI particles from the HN(B656) mutant is consistently about 2 times longer (65 ± 10 ps) than that observed in the wild type. The antenna size of different PSI preparations showed some variability. However, the data of Table 1 show that differences in trapping times between wild type and mutant PSI are much larger than differences

Table 1: Trapping Times Obtained by Global Analysis of Time-Resolved Transient Absorption Data for Different PSI Particles Isolated from Wild Type and HN(B656) Mutant of *C. reinhardtii* (λ_{exc} = 700 nm)

type of PSI	Chl *a*/P_{700} ratio	trapping time (ps) (mean ± SD)
1. wild type[a]	100	30 ± 5
2. wild type[b]	60	24
3. wild type[b]	45	25 ± 4
4. wild type,[c] Chl *b*-less	30	21 ± 3
5. HN(B656)[b]	80	62 ± 8
6. HN(B656)[b]	60	72 ± 10

[a] β-DM-isolated particles. [b] Triton X-100-isolated particles (see Materials and Methods). [c] TX100-isolated particles from PSII-less Chl *b*-less strain 2696 of *C. reinhardtii*. Data were obtained on both 90- and 180-ps time scales and are presented as mean ± SD from different global analysis fits within each data set.

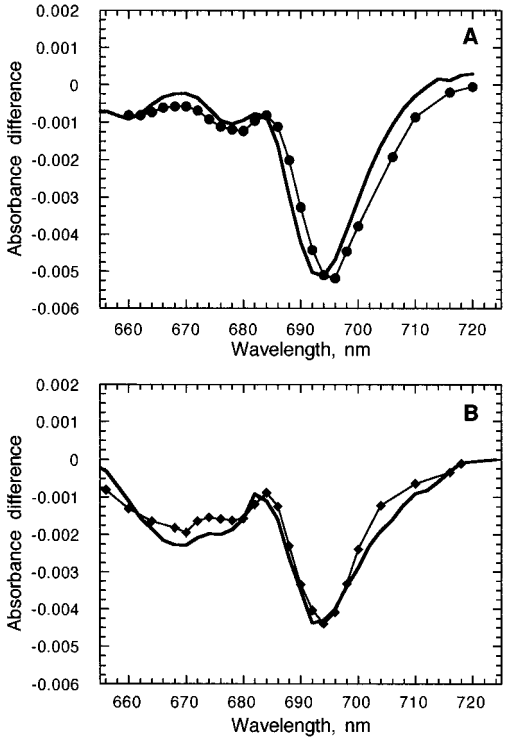

FIGURE 3: Comparison of DAS of nondecaying components obtained by global analysis of time-resolved absorption kinetics measured under neutral conditions (solid lines) with the difference spectra ($P_{700}^+ - P_{700}$) measured after saturating laser flash excitation on the millisecond time scale (closed symbols) for detergent-isolated wild type (A) and HN(B656) mutant (B) PSI. The millisecond spectra are normalized at 694 nm for ease of comparison. The new band at 670 nm appears in the spectra of HN(B656) PSI.

due to antenna size (trapping time is nearly independent of antenna size in both PSI preparations).

For both wild type and HN(B656) mutant PSI, we measured the flash-induced spectra of P_{700} oxidation on a millisecond time scale. The difference spectrum $P_{700}^+ - P_{700}$ of wild type PSI (Figure 3A; closed symbols) shows a photobleaching band at 695 nm ascribed to the formation of P_{700}^+ and a photobleaching band at 680 nm possibly reflecting an electrochromic shift of an absorption band of Chl *a* molecules in response to formation of P_{700}^+. The difference spectrum $P_{700}^+ - P_{700}$ of the mutant PSI (Figure 3B; closed symbols) also shows the photobleaching at 694 and 680 nm. However, a new band at 670 nm appears. A similar difference spectrum ($P_{700}^+ - P_{700}$) for the HN(B656) TX100-isolated PSI was reported recently (Webber et al., 1996). The comparison of nondecaying components in Figure 2A and Figure 2B with millisecond spectra normalized at 694 nm (Figure 3A,B) shows that the shape of the nondecaying spectra for both PSI particles is in good agreement with the shape of the millisecond spectra measured under neutral conditions for both PSI particles. Small differences are probably associated with the noise from different instruments. Since the millisecond spectrum in Figure 3B reflects the photooxidation of P_{700} and possible electrochromic shifts of a neighboring Chls' absorption band due to formation of P_{700}^+, we can ascribe the nondecaying spectrum in Figure 3B to the formation of P_{700}^+ and possible electrochromic shifts.

Transient Absorption Measurements under Reducing Conditions. Highly reducing conditions were described under Materials and Methods. Under these conditions, the doubly reduced molecule of the secondary electron acceptor, A_1, blocks further electron transport in the RC. Therefore, the transient absorption spectra of PSI reaction centers on the picosecond time scale should represent antenna changes and changes associated with photooxidation of P_{700} and photoreduction of A_0. For each set of experiments with PSI preparations both from wild type and from the HN(B656) mutant, the data were collected on a 90-ps time scale using low excitation intensities similar to those used for neutral conditions.

Figure 4A shows the nondecaying spectra obtained by the global analysis of transient absorption spectra measured in the wild type PSI both under neutral and under reducing conditions. This component for reducing conditions is characterized by a broad photobleaching with a peak at 688 nm and a broad shoulder at 670 nm. Figure 4C displays the spectra of the nondecaying components obtained by the global analysis of time-resolved spectra of the HN(B656) mutant of PSI both under neutral and under reducing conditions. The nondecaying spectrum obtained under reducing conditions in the mutant PSI is broader than that in the wild type PSI, indicating the contribution of photobleaching at 670 nm into the mutant spectrum taken under reducing conditions.

It was shown above that nondecaying spectra of open PSI reaction centers from both wild type and the HN(B656) mutant in the 650−730 nm spectral region are due to formation of P_{700}^+ (Figure 3A,B). Nondecaying spectra of PSI obtained under reducing conditions are most likely due to $P_{700}^+A_0^-$, which is known to decay in about 30−50 ns (Mathis et al., 1988; Sétif & Bottin, 1989; Kleinherenbrink et al., 1994). Subtraction of the nondecaying spectrum associated with P_{700}^+ from the nondecaying spectrum obtained from transient absorption spectra measured under reducing conditions ($P_{700}^+A_0^-$) gives the spectrum associated with the photoreduction of the primary acceptor molecule A_0. Figure 4B,D displays the result of such a subtration for wild type and HN(B656) mutant PSI. For the mutant PSI, several different normalization factors of the $P_{700}^+ - P_{700}$ difference spectrum were used before its subtraction from the nondecaying spectrum was measured under reducing conditions. Such a procedure was used earlier to obtain A_0 photoreduction spectra in PSI from spinach and is needed because slight differences in sample concentrations and laser intensities cause small differences in the amount of charge-separated state generated in the different samples (Hastings

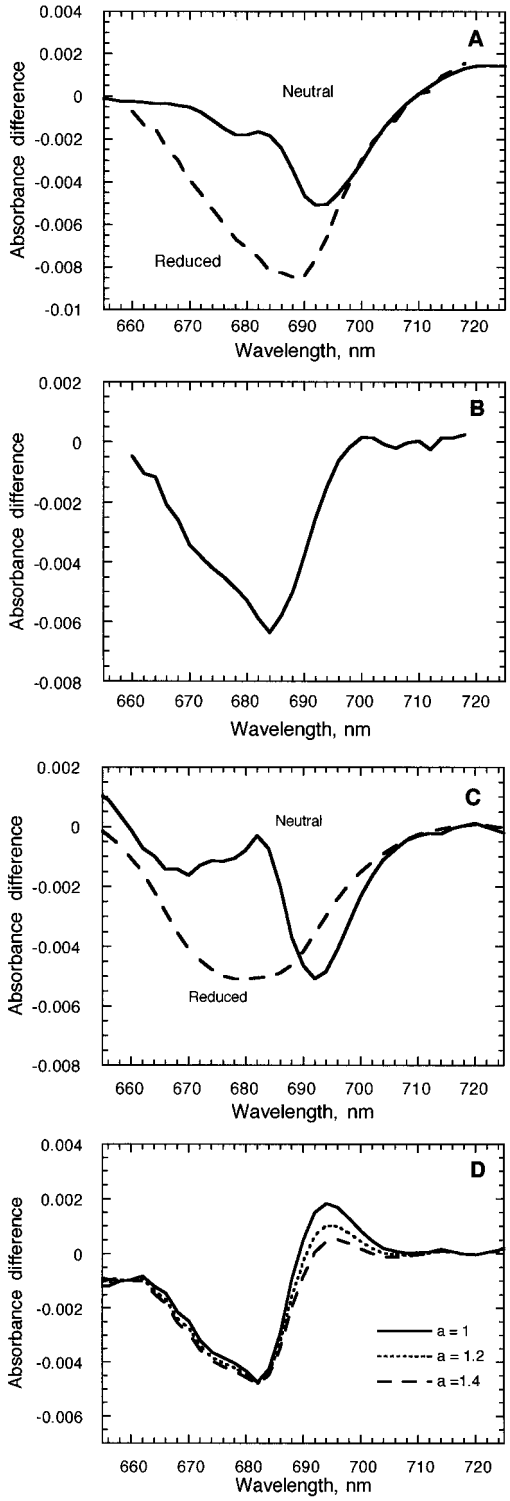

FIGURE 4: (A and C) Nondecaying spectra obtained from the global analysis of data measured under neutral (—) and reducing (- - -) conditions for detergent-isolated PSI from wild type (A) and HN-(B656) mutant (C) of *C. reinhardtii*. (B and D) Difference spectra obtained by subtraction of the P_{700} spectrum (nondecaying spectrum under neutral conditions) from the nondecaying spectrum obtained under reducing conditions for wild type (B) and HN(B656) mutant PSI (D). In panel D, the spectra are obtained by subtraction of the P_{700} oxidation spectrum of the mutant PSI using different normalization factors designated as "a".

et al., 1995a). Figure 4D shows that the shape of the A_0 photoreduction spectrum in the 660−690 nm spectral region and the position of the maxima of photobleaching at 682 nm are nearly independent of normalization factors. The spectrum in Figure 4B and the spectrum obtained with normalization factor of 1.4 in Figure 4D are similar in shape. The differences in photobleaching maxima are within the wavelength resolution. Both spectra are characterized by an asymmetric form due to contributions from absorbance changes around 670 nm. The spectra of the primary acceptor photoreduction with similar shapes were reported earlier for PSI from green algae and cyanobacteria (Hastings et al., 1995a) and higher plants (Shuvalov et al., 1986; Kumazaki et al., 1995a,b; Hastings et al., 1995a). The similarity of spectra in Figure 4B and Figure 4D implies that similar processes occur in the RC of PSI from wild type and HN-(B656) mutant.

Table 2: Comparison of Time-Resolved Fluorescence of PSI Isolated from Wild Type and HN(B656) Mutant of *C. reinhardtii*[a]

type of PSI	Chl *a*/P_{700} ratio	parameter	lifetimes (ps) and relative amplitudes (%) of exponential components, i = 1	2	3
		λ_{exc} = 590 nm; λ_{em} = 700 nm			
1. wild type[b]	100	λ_i	30	296	1932
		A_i	96	3	1
2. HN(B656)[c]	60	τ_i	68	573	2614
		A_i	70	24	6
		λ_{exc} = 682 nm; λ_{em} = 700 nm			
3. wild type[b]	100	τ_i	25	184	1735
		A_i	95	4	1
4. wild type[c]	45	τ_i	28	384	2638
		A_i	87	9	4
5. HN(B656)[c]	60	τ_i	74	463	2474
		A_i	75	20	5

[a] Fluorescence decay kinetics were fitted to a sum of exponentials: $\sum A_i \exp(-t/\tau_i)$, where A_i is the initial amplitude of the ith component and τ_i is the lifetime of the ith component. For all fits, the χ^2 parameter was less than 1.15. [b] β-DM-isolated particles. [c] TX100-isolated particles (see Materials and Methods).

Single-Photon Counting Measurements. Experiments using picosecond fluorescence spectroscopy have been performed to obtain independent evidence of the rate of the trapping process in the PSI core from the site-directed HN-(B656) mutant. For single-photon counting measurements, we used PSI preparations both of wild type and of HN(B656) mutant isolated in the presence of the detergents β-DM or TX100. Under our experimental conditions, reaction centers were in the closed (P_{700} oxidized) state (see Materials and Methods), so that the measured fluorescence originated from only the excited states of Chl *a* in the antenna. We also took into account the previously reported facts that the kinetics of PSI fluorescence decay are independent of the redox state of RC (Owens et al., 1988; Turconi et al., 1993; Hastings et al., 1994a).

The fluorescence decay kinetics in different PSI preparations at different emission wavelengths were fit to a sum of exponential components. The results of the three-component fit obtained for data measured at 700 nm emission wavelength and excitation at 590 and 682 nm for PSI particles with different antenna size are presented in Table 2. Fluorescence decay of wild type PSI is dominated by a fast component with a lifetime of ~30 ps and ~95% of the initial amplitude of the decay. The fast component of fluorescence decay in antenna of PSI from the HN(B656) mutant of *C. reinhardtii* has a lifetime of ~65 ps and ~75% of the initial amplitude.

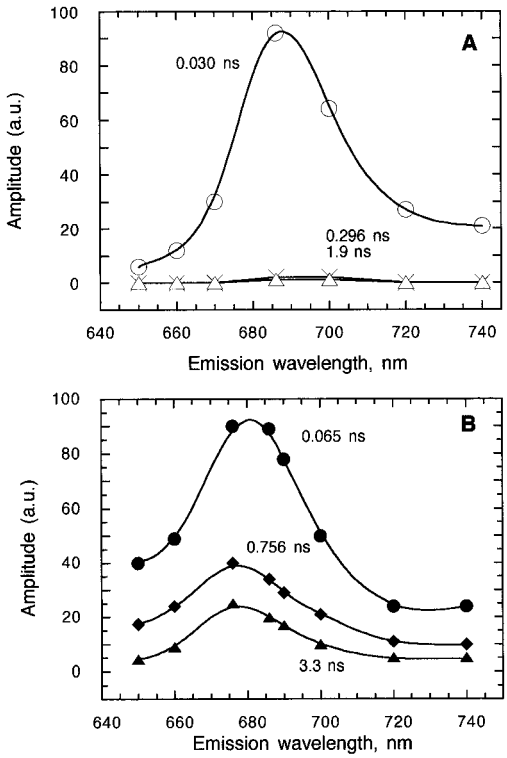

FIGURE 5: Fluorescence decay-associated spectra obtained from a three-component global fit of the fluorescence decays upon excitation at 590 nm at room temperature for detergent-isolated PSI from wild type (A) and HN(B656) mutant (B) of *C. reinhardtii*.

The DAS obtained by global analysis of data measured for PSI from the wild type and HN(B656) mutant of *C. reinhardtii* using laser excitation at 590 nm are given in Figure 5A,B. The shapes of the spectra of the dominating fast components both in PSI from wild type and in the HN(B656) mutant are similar to the shape of the 30-ps DAS and the 65-ps DAS in Figure 2A,B, indicating that these spectra reflect similar processes in the PSI antenna, trapping of antenna excitation by the reaction center. The data of Figure 5B and Table 2 show that increased amplitudes of intermediate components in mutant PSI do not affect the lifetime of the fast decay component. From a comparison of the amplitudes of these components in different PSI preparations, we suggest that the slower components are associated with detergent treatment. Our data also show that the presence of Chl *b* in PSI preparations does not affect the lifetimes of the processes studied here. This is consistent with the result shown earlier that energy transfer from Chl *b* to the PSI core antenna takes <5 ps (Owens et al., 1988).

Figure 6 displays a comparison of the fast decay components in PSI from wild type and the HN(B656) mutant of *C. reinhardtii* at different emission wavelengths. The data clearly show that the lifetime of the trapping process in the HN(B656) mutant PSI (62 ± 15 ps) is approximately 2 times longer than that in the wild type PSI (29 ± 8 ps). The trapping time of the PSI antenna in wild type and the mutant is almost independent of emission wavelength within experiment error.

DISCUSSION

Overall Decay and Trapping in PSI from Wild Type and HN(B656) Mutant. Measurements of flash-induced absorbance changes and charge recombination kinetics on the

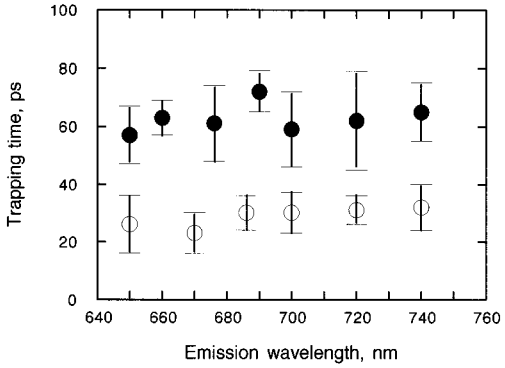

FIGURE 6: Trapping times in detergent-isolated PSI preparations of wild type (open symbols) and HN(B656) mutant (closed symbols) of *C. reinhardtii* at different emission wavelengths. Data were obtained from time-correlated single-photon counting. THe excitation wavelength was at 590 nm. The error bars represent the standard errors of both different fits and independent measurements on different preparations.

millisecond time scale (data not shown) revealed that our preparations of both wild type and mutant PSI contain a full set of acceptors transferring electrons from the primary donor to iron−sulfur centers. Good agreement of the spectral shapes and lifetimes of decay components with those obtained earlier for TX100-isolated PSI from cyanobacteria, higher plants, and β-DM-isolated PSI from *C. reinhardtii* (Hastings et al., 1995a,b) suggests that our preparations are relatively intact.

The fact that the shape of the transient absorption spectrum measured at 4-ps time delay in the wild type PSI (Figure 1A) is very similar to that measured for the mutant PSI (Figure 1B) implies that similar processes of initial excitation dynamics occur in the core antenna of both PSI particles. The 4-ps DAS revealed under excitation at 700 nm for the wild type PSI (Figure 2A) indicates the presence of the faster energy transfer processes in the antenna. The shape of this kinetic component is characteristic of the uphill energy transfer from long-wavelength-absorbing pigments to pigments absorbing around 680 nm. We were unable to resolve this fast component in the mutant PSI antenna decay, although the time scales of the experiments were not optimized for detection of this kinetic phase.

Comparison of transient absorption spectra measured for PSI from the wild type and HN(B656) mutant of *C. reinhardtii* (Figures 1 and 2) reveals some differences in the mutant spectra that we attribute to changes caused by the HN(B656) mutation. The 70-ps spectrum in the mutant PSI (Figure 1B) represents an ongoing process in the antenna while the 70-ps spectrum in the wild type PSI (Figure 1A) reflects a state that is nondecaying on the time scale considered here and appears to be indicative of absorbance changes of P_{700}, i.e., primary charge separation in the RC. Transient absorption spectra measured at 30 ps in the wild-type PSI and at 70 ps in the mutant PSI may have some contributions from absorbance changes of the primary acceptor A_0 in RC. However, the intermediate transient concentration of the reduced acceptor following low intensity excitation in open RCs is very low (Hastings et al., 1995a).

To distinguish between overlapping PSI core antenna and RC processes, we performed global analysis of transient absorption spectra (Figure 2A,B). We used in our experiments PSI isolated both from Chl *b*-containing and from Chl *b*-less (data not shown) strains of *C. reinhardtii* and found

the fast components of transient absorption changes with lifetimes of 30 and 21 ps, respectively, for PSI from Chl *b*-containing and Chl *b*-less strains. The shape of the DAS of these components is similar to the shape of the same DAS for PSI from the Chl *b*-less strain of *C. reinhardtii* reported earlier (Hastings et al., 1995a) and for cyanobacterial (Hastings et al., 1994a, 1995a,b; Turconi et al., 1993) and spinach PSI (Holzwarth et al., 1993; Hastings et al., 1995a). This comparison clearly shows that the presence of peripheral antenna Chl *b* in our preparations does not significantly affect the primary excited state dynamics in PSI core antenna upon excitation at 700 nm. Both time-resolved transient absorption and fluorescence spectroscopy assigned the component of the PSI antenna decaying with lifetimes 20−30 ps to the trapping process from the relaxed state following the faster (∼2−8 ps) equilibration process in the spectrally inhomogeneous PSI antenna (Klug et al., 1989; Holzwarth et al., 1993; Hastings et al., 1994a, 1995a,b; DiMagno et al., 1995).

The 30- and 65-ps DAS in Figure 2A,B have similar shapes but different lifetimes, 26 ± 5 ps and 65 ± 10 ps, respectively, for the wild type and the mutant PSI (see also Table 1). This similarity of the spectral profile and difference in the lifetimes of these components is a very important point. First, it shows that the 30- and 65-ps DAS represent the trapping process in PSI core antenna. Second, it implies that both PSI have a similar spectral distribution of the antenna pigments and substitution of His-656 by Asn near the P_{700} molecule is a localized mutation that probably does not affect the structure of the core antenna in the mutant PSI. This supports our conclusion that slowing of the trapping process in the mutant PSI is a result of the altered properties of P_{700} due to the mutation.

Time-resolved measurements of PSI antenna fluorescence decay in both PSI particles provide independent evidence that the trapping processes in the wild type and the mutant PSI have different lifetimes. Comparisons of the DAS of the fast dominating components of antenna decay in the wild-type and mutant PSI in Figure 5A,B and the 30-ps and 65-ps DAS in Figure 2A,B show that these spectra represent the same trapping process in the PSI antenna with the lifetime for the HN(B656) mutant PSI (62 ± 15 ps) being 2 times longer than that in the wild type PSI (29 ± 8 ps) (Table 2).

Webber et al. (1996) showed recently that mutation of His-656 to Asn or Ser increases the midpoint redox potential of P_{700}/P_{700}^+ by 40 mV. The 4.0−4.5 Å resolution X-ray structure of cyanobacterial PSI (Krauss et al., 1996) revealed the presence of monomeric Chls, one of which is probably the primary acceptor molecule A_0. As the site of the mutation is relatively far from the electron acceptor molecule in PSI, we can assume that the free energy of the primary charge-separated state is increased in our mutants in proportion to the changes in E_m of P as it was assumed for purple bacteria (Nagarajan et al., 1993). An increase in the midpoint potential led to a decrease in the free energy between P* and $P^+H_L^-$ (the primary charge-separated state in RC of purple bacteria) followed by a decrease of the electron transfer rate from P and H_L (Woodbury & Allen, 1995). However, experiments for membrane complexes of antenna and RC from purple bacteria revealed that amino acid substitutions near the primary donor have only a slight effect on the rate of energy transfer from antenna to RC (Beekman et al., 1994). It was concluded that the limiting step of the trapping process in the antenna of purple bacteria is energy transfer from antenna to the RC; i.e., the energy transfer is migration (diffusion)-limited (Beekman et al., 1994; Sundström & van Grondelle, 1995).

Based on our experiments, we come to quite a different conclusion for PSI. On the first hand, our data show that the PSI core antenna from the HN(B656) mutant is probably unaffected by the mutation. On the second hand, the trapping time in the HN(B656) PSI is about 2 times longer than in the wild type PSI. We think that these facts suggest that the trapping process in the mutant is limited by the charge separation kinetics in the PSI RC because changes in the trap (P_{700}) cause changes in the trapping time. This is consistent with the trap-limited model of excitation dynamics in PSI (Pearlstein, 1982; Trissl, 1993). It would be expected that the HN(B656) mutation near P_{700} resulting in an increased midpoint potential would decrease the rate of electron transfer between P_{700} and the primary acceptor A_0. It is difficult to measure the primary charge separation kinetics directly in PSI. However, we can estimate the upper limit for the rate of radical pair formation in PSI RCs from wild type and the HN(B656) mutant of *C. reinhardtii* using the equation given by Trissl (1993) and the trapping times measured in this work. Taking into account that the number of red pigments in PSI from *C. reinhardtii* was estimated to be ∼2 (Werst et al., 1992) and that our particles contain ∼60 Chl molecules per P_{700}, we can estimate the effective antenna size as about 13 and the upper limits of charge separation times for wild type and the mutant as 1.5 and 3.5 ps, respectively.

Because we have no direct experimental evidence that the rate of the primary charge separation process in HN(B656) PSI is decreased, we cannot exclude another explanation of the slowing of the trapping process in the mutant based on the special trap-limited model proposed for purple bacteria (van Grondelle & Sundström, 1988; Otte et al., 1993). According to this model, the trapping is limited by the process of energy transfer from the red pigments to the trap. If these molecules are coupled to P_{700} as was assumed earlier (Gobets et al., 1994), then specific mutations near the primary donor that shift the midpoint potential of P_{700} may result in a change of the lifetime of the trapping process. It should be noted that recent refinement of the PSI structure model revealed the presence of another two Chls (additional to six found earlier) bridging the Chls of the RC with the PSI core antenna Chls (Krauss et al., 1996). It is interesting to speculate that these Chls might serve as red pigments in PSI.

P_{700} Photooxidation in PSI from Wild Type and HN(B656) Mutant. Once the PSI antenna excitation is trapped, it initiates the charge separation in the PSI RC. In open RCs, the chain of electron acceptors mediates electron transfer to iron−sulfur centers that stabilizes the charge separation. The primary acceptor molecule A_0 and accessory Chl molecules revealed by the X-ray structure probably absorb in the same spectral region as P_{700}. However, under neutral conditions and low intensity illumination, the transient concentration of the primary reduced acceptor is decreased (Hastings et al., 1995a), and absorbance changes reflect mainly formation of P_{700}^+. The comparison of the nondecaying components obtained from global analysis of time-resolved spectra of both wild type and HN(B656) mutant PSI with $P_{700}^+ - P_{700}$ difference spectra measured on a millisecond time scale (Figure 3A,B) clearly shows that the nondecaying components of transient absorption spectra of both the wild type

and the mutant PSI are due to absorbance changes accompanying the formation of P_{700}^+.

Evidently, substitution of His-656 for Asn leads to a significant change in the P_{700} difference spectrum (see spectra of ND DAS in Figures 2B and 3B). If His-656 is a ligand to P_{700}, then the appearance of a new band in the P_{700} difference spectrum of the mutant PSI could reflect at least two possibilities. First, substitution of His by Asn could change the exciton interaction in P_{700} and lead to the appearance of the high-energy exciton component of P_{700} at 670 nm. This possibility for HN(B656) PSI was suggested recently by Webber et al. (1996). Second, the mutation could induce the electrochromic shift in absorption of neighboring Chls in response to formation of P_{700}^+. It is known that 670 nm is a Qy transition for the Chl *a* monomer (Fujita et al., 1978). ENDOR spectra of the mutant PSI measured by Webber et al. (1996) revealed different spin distribution in wild type and the mutant P_{700}. A larger extent of the spin density localization on half of the mutated dimer can result in an electrochromic shift of the absorption band of neighboring Chl *a* monomers around 670 nm. However, we cannot exclude the possibility that His-656 is a ligand to a neighboring Chl. The 4−4.5 Å resolution X-ray study of cyanobacterial PSI (Fromme et al., 1996; Krauss et al., 1996) revealed the presence of at least four additional Chl molecules near P_{700}. Two of them are located in close proximity to the special pair. In this case, a new band at 670 nm in the P_{700} difference spectrum of the mutant PSI could also be due to an electrochromic shift in the absorption of a mutated Chl *a* molecule neighboring P_{700}.

Figures 1 and 2 reveal another spectroscopic change possibly caused by the mutation. The ratio of the photobleaching maximum in the spectrum of the fast decaying component to that of the nondecaying spectrum in the HN(B656) mutant PSI is higher than in the wild type PSI. It can be suggested that in mutant PSI a portion of the excited state of P_{700} decays via a radiationless pathway possibly due to vibrational interaction of the special pair molecule with the surrounding mutated protein. Another possible explanation is that the differential extinction coefficient of P_{700} is changed due to the mutation.

Photoreduction of the Primary Acceptor. The similarity of $A_0^- - A_0$ difference spectra both in the mutant and in wild type PSI (Figure 4B,D) indicates that photoreduction of A_0 in the mutant PSI is a similar process to the wild type PSI and substitution of His for Asn at the 656th position of PsaB near P_{700} molecule does not significantly affect the properties of the primary electron acceptor molecule A_0.

The similar shape of the A_0 photoreduction spectrum was reported earlier for spinach PSI (Shuvalov et al., 1986; Kumazaki et al., 1994a,b; Hastings et al., 1995a) and for PSI from Chl *b*-less *C. reinhardtii* (Hastings et al., 1995a). The possible explanation of the broad shoulder at 670 nm in the $A_0^- - A_0$ difference spectrum [see Hastings et al. (1995a) and references cited therein] involves the consideration of additional pigments in the vicinity of P_{700} and A_0 shown recently by the crystal structure of cyanobacterial PSI (Fromme et al., 1996; Krauss et al., 1996). Therefore, it may be more correct to ascribe the spectrum of A_0 photoreduction to a spectrum of photoreduction of a primary acceptor complex, that may involve more than one Chl molecule.

CONCLUSIONS

The data presented in this paper provide further spectroscopic evidence that His-656 in PsaB is probably a ligand to P_{700}. The substitution of this His for Asn results in significant changes of both antenna trapping time and spectroscopic properties of P_{700}.

It is likely that the HN(B656) mutation does not affect the structure of the PSI core antenna as the shape of the spectrum reflecting the energy transfer from antenna to RC in the mutant PSI is similar to that in the wild type PSI. The PSI core from the HN(B656) mutant of *C. reinhardtii* has a trapping time about 2 times longer than in the wild type PSI. The fact that substitution of His-656 of PsaB in the close vicinity of P_{700} for Asn in PSI results in increasing the excited state lifetime in the RC apparently implies that the bottleneck of the trapping process is the primary charge separation. The estimated upper values for the primary charge separation time in both wild type and HN(B656) mutant PSI based upon a trap-limited model of excitation dynamics are 1.5 and 3.5 ps, respectively.

In open PSI RCs, the trapping process results in charge separation, and the absorption difference spectrum of this state is due to formation of P_{700}^+ both in the wild type and in HN(B656) mutant PSI. However, a new band at 670 nm appears in the P_{700} oxidation spectrum of the mutant. We suggest that this band reflects either changed exciton interaction within the dimer caused by the replacement of His-656 by Asn or electrochromic shift of the absorption band of Chls located in close proximity to P_{700}.

The $A_0^- - A_0$ difference spectrum in the mutant PSI resembles the same spectrum from the wild type RC. This suggests that mutation does not affect the properties of the primary electron acceptor molecule in PSI.

ACKNOWLEDGMENT

We thank Dr. Christian Poweleit for his assistance with the time-resolved fluorescence measurements.

REFERENCES

Beekman, L. M. P., van Mourik, F., Jones, M. R., Visser, H. M., Hunter, C. N., & van Grondelle, R. (1994) *Biochemistry 33*, 3143−3147.

Bennoun, P. M., Spierer-Herz, J., Erickson, J., Girard-Bascou, J., Pierre, Y., Delsòme, M., & Rochaix, J.-D. (1986) *Plant. Mol. Biol. 6*, 151−160.

Causgrove, T. P., Brune, D. C., Blankenship, R. E., & Olson, J. M. (1990) *Photosynth. Res. 25*, 1−10.

Cui, L., Bingham, S. E., Kuhn, M., Kass, H., Lubitz, W., & Webber, A. N. (1995) *Biochemistry 34*, 1549−1558.

DiMagno, L., Chan, C. K., Jia, Y. W., Lang, M. J., Newman, J. R., Mets, L., Fleming, G. R., & Haselkorn, R. (1995) *Proc. Natl. Acad. Sci. U.S.A. 92*, 2715−2719.

Du, M., Xie, X., Jia, Y., Mets, L., & Fleming, G. R. (1993) *Chem. Phys. Lett. 201*, 535−542.

Fromme, P., Witt, H. T., Schubert, W.-D., Klukas, O., Saenger, W., & Krauss, N. (1996) *Biochim. Biophys. Acta 1275*, 76−83.

Fujita, I., Davis, M. S., & Fajer, J. D. (1978) *J. Am. Chem. Soc. 100*, 6280−6282.

Gobets, B., van Amerongen, H., Monshouwer, R., Kruip, J., Rögner, M., van Grondelle, R., & Dekker, J. P. (1994) *Biochim. Biophys. Acta 1188*, 75−85.

Golbeck, J. H., & Bryant, D. A. (1991) *Curr. Top. Bioenerg. 16*, 83−175.

Hastings, G., Kleinherenbrink, A. M., Lin, S., & Blankenship, R. E. (1994a) *Biochemistry 33*, 3185−3192.

Hastings, G., Kleinherenbrink, F. A. M., Lin, S., McHugh, T. J., & Blankenship, R. E. (1994b) *Biochemistry 33*, 3193−3200.
Hastings, G., Hoshina, S., Webber, A. N., & Blankenship, R. E. (1995a) *Biochemistry 34*, 15512−15522.
Hastings, G., Reed, L. J., Lin, S., & Blankenship, R. E. (1995b) *Biophys. J. 69*, 2044−2055.
Hecks, B., Wulf, K., Breton, J., Leible, W., & Trissl, H.-W. (1994) *Biochemistry 33*, 8619−8624.
Hiyama, T., & Ke, B. (1972) *Arch. Biochem. Biophys. 147*, 99−108.
Holzwarth, A. R., Schatz, G. H., Brock, H., & Bittersmann, E. (1993) *Biophys. J. 64*, 1813−1826.
Kleinherenbrink, F. A. M., Hastings, G., Wittmershaus, B., & Blankenship, R. E. (1994) *Biochemistry 33*, 3096−3105.
Klug, D. R., Giorgi, L. B., Crystal, B., Barber, J., & Porter, G. (1989) *Photosynth. Res. 22*, 277−284.
Krabben, L., Käss, H., Schlodder, E., Kuhn, M., Lubitz, W., Xu, H., Bingham, S., & Webber, A. (1995) in *Photosynthesis: from Light to Biosphere* (Mathis, P., Ed.) Vol. II, pp 123−126, Kluwer Academic Publishing, Dordrecht, The Netherlands.
Krauss, N., Schubert, W.-D., Klukas, O., Fromme, P., Witt, H. T., & Saenger, W. (1996) *Nat. Struct. Biol. 3*, 965−973.
Kumazaki, S., Kandori, H., Petek, H., Ikegami, I., Yoshihara, K., & Itoh, S. (1994a) *J. Phys. Chem. 98*, 10335−10342.
Kumazaki, S., Iwaki, M., Ikegami, I., Kandori, H., Yoshihara, K., & Itoh, S. (1994b) *J. Phys. Chem. 98*, 11220−11225.
Laible, P. D., Zipfel, W., & Owens, T. G. (1994) *Biophys. J. 66*, 844−860.
Lin, S., Chiou, H.-C., & Blankenship, R. E. (1995) *Biochemistry 34*, 12761−12767.
Mathis, P., Ikegami, I., & Sétif, P. (1988) *Photosynth. Res. 16*, 203−210.
Moënne-Loccoz, P., Heathcote, P., Maclachlan, D. J., Berry, M. C., Davis, I. H., & Evans, M. C. W. (1994) *Biochemistry 33*, 10037−10042.
Nagarajan, V., Parson, W. W., Davis, D., & Schenck, G. C. (1993) *Biochemistry 32*, 12324−12336.
Otte, S. C. M., Kleinherenbrink, F. A. M., & Amesz, J. (1993) *Biochim. Biophys. Acta 848*, 193−200.
Owens, T. G., Webb, S. P., Alberte, R. S., & Fleming, G. R. (1988) *Biophys. J. 53*, 733−745.
Pearlstein, R. M. (1982) in *Photosynthesis* (Govindjee, Ed.) pp 293−330, Academic Press, New York.
Sétif, P., & Bottin, H. (1989) *Biochemistry 28*, 2689−2697.
Shuvalov, V. A., Nuijs, A. M., van Gorkom, H. J., Smit, H. W. J., & Duysens, L. N. M. (1986) *Biochim. Biophys. Acta 850*, 319−323.
Sundström, V., & van Grondelle, R. (1995) in *Anoxygenic Photosynthetic Bacteria* (Blankenship, R. E., Madigan, M. T., & Bauer, S. E., Eds.) pp 349−372, Kluwer Academic Publishing, Dordrecht, The Netherlands.
Takahashi, Y., Goldschmidt-Clermont, M., Soen, S. Y., Franzen, L. G., & Rochaix, J. D. (1991) *EMBO J. 10*, 2033−2040.
Thornber, J. P. (1969) *Biochim. Biophys. Acta 172*, 230−241.
Trissl, H.-W. (1993) *Photosynth. Res. 35*, 247−263.
Turconi, S., Schweitzer, G., & Holzwarth, A. R. (1993) *Photochem. Photobiol. 57*, 113−119.
van Grondelle, R., & Sundström, V. (1988) in *Photosynthetic Light Harvesting Systems* (Scheer, H., & Schneider, S., Eds.) pp 403−438, Gruyter, Berlin.
Webber, A. N., Su Hui, Bingham, S. E., Kass, H., Krabben, L., Kuhn, M., Jordan, R., Schlodder, E., & Lubitz, W. (1996) *Biochemistry 35*, 12857−12863.
Werst, M. M., Jia, Y., Mets, L., & Fleming, G. R. (1992) *Biophys. J. 61*, 868−878.
White, N. T. H., Beddard, G. S., Thorne, J. R. G., Feehan, T. M., Keyes, T. E., & Heathcote, P. (1996) *J. Phys. Chem. 100*, 12086−12099.
Woodbury, N., & Allen, J. (1995) in *Anoxygenic Photosynthetic Bacteria* (Blankenship, R. E., Madigan, M. T., & Bauer, S. E., Eds.) pp 527−557, Kluwer Academic Publishing, Dordrecht, The Netherlands.

BI962235M